Clim. Past, 9, 955–968, 2013
www.clim-past.net/9/955/2013/
doi:10.5194/cp-9-955-2013
© Author(s) 2013. CC Attribution 3.0 License.

Climate of the Past
Open Access

Model sensitivity to North Atlantic freshwater forcing at 8.2 ka

C. Morrill[1,2], A. N. LeGrande[3], H. Renssen[4], P. Bakker[4], and B. L. Otto-Bliesner[5]

[1]Cooperative Institute for Research in Environmental Sciences, University of Colorado, Boulder, CO, USA
[2]National Oceanic and Atmospheric Administration's National Climatic Data Center, Boulder, CO, USA
[3]NASA Goddard Institute for Space Studies and Center for Climate Systems Research, New York, NY, USA
[4]Department of Earth Sciences, VU University Amsterdam, the Netherlands
[5]Climate and Global Dynamics, National Center for Atmospheric Research, Boulder, CO, USA

Correspondence to: C. Morrill (carrie.morrill@colorado.edu)

Received: 31 July 2012 – Published in Clim. Past Discuss.: 21 August 2012
Revised: 12 March 2013 – Accepted: 13 March 2013 – Published: 10 April 2013

Abstract. We compared four simulations of the 8.2 ka event to assess climate model sensitivity and skill in responding to North Atlantic freshwater perturbations. All of the simulations used the same freshwater forcing, 2.5 Sv for one year, applied to either the Hudson Bay (northeastern Canada) or Labrador Sea (between Canada's Labrador coast and Greenland). This freshwater pulse induced a decadal-mean slowdown of 10–25 % in the Atlantic Meridional Overturning Circulation (AMOC) of the models and caused a large-scale pattern of climate anomalies that matched proxy evidence for cooling in the Northern Hemisphere and a southward shift of the Intertropical Convergence Zone. The multi-model ensemble generated temperature anomalies that were just half as large as those from quantitative proxy reconstructions, however. Also, the duration of AMOC and climate anomalies in three of the simulations was only several decades, significantly shorter than the duration of ∼150 yr in the paleoclimate record. Possible reasons for these discrepancies include incorrect representation of the early Holocene climate and ocean state in the North Atlantic and uncertainties in the freshwater forcing estimates.

1 Introduction

The Atlantic Meridional Overturning Circulation (AMOC) plays a key role in the climate system, particularly through its control on heat transport and storage of carbon in the deep ocean. Changes in the AMOC can have far-reaching effects on the El Niño–Southern Oscillation (Timmermann et al., 2005), Atlantic hurricane development (Zhang and Delworth, 2006), tropical rainfall (Vellinga and Wood, 2002), and marine ecosystems (Schmittner, 2005). Model simulations of the 21st century with prescribed greenhouse gas concentrations increasing according to the Intergovernmental Panel on Climate Change (IPCC) scenario SRESA1B uniformly show a reduction in the strength of the AMOC (Schmittner et al., 2005). This multi-model ensemble yields a mean decrease of 25 % by 2100, but there is a large range in the individual model results that indicates substantial uncertainties in the AMOC response to climate change.

Several previous model intercomparison projects were undertaken to improve understanding of the large spread in modeled AMOC. Schmittner et al. (2005) considered the skill of nine coupled climate models in matching observations of modern hydrography. They found that the models were more successful at reproducing temperature patterns than either salinity patterns or pycnocline depth. Stouffer et al. (2006) examined the response of both Earth system models of intermediate complexity (EMICs) and coupled atmosphere–ocean general circulation models (AOGCMs) to North Atlantic freshwater forcings of 0.1 and 1.0 Sv (Sverdrup $= 10^6\ m^3\ s^{-1}$) for 100 yr. While there were some robust patterns among the models, important disagreements existed in model sensitivity and in reversibility following AMOC shutdown. Since these were idealized experiments, no comparison to observations was possible. Otto-Bliesner et al. (2007) compared AMOC in four Last Glacial Maximum simulations from the second phase of the Paleoclimate Modelling Intercomparison Project (PMIP2). These models gave very different glacial circulations and a comparison to

Table 1. Participating models.

Model	Atmospheric model	Oceanic model	Citations
CCSM3	CAM3: T42 (∼ 2.8 × 2.8°), 26 levels	POP: ∼ 1× ∼ 1°; ∼ 0.3× ∼ 0.3° in North Atlantic, 40 levels, volume-conserving	Collins et al. (2006) Otto-Bliesner et al. (2006) Wagner et al. (2013)
GISS ModelE-R	ModelE: M20 (4×5°), 20 levels	Russell: 4 × 5°, 13 levels, mass-conserving	Schmidt et al. (2006) Russell et al. (2000, 1995) LeGrande et al. (2006) LeGrande and Schmidt (2008)
LOVECLIM1.2	ECBilt2: T21 (5.625 × 5.625°), 3 levels	CLIO3: 3 × 3°, 20 levels, mass-conserving	Goosse et al. (2010)

paleoclimate proxy evidence indicated serious mismatches for several of the simulations.

For the third phase of PMIP, the 8.2 ka event has been targeted for a new model intercomparison. Of past abrupt changes in the AMOC, the 8.2 ka event provides a particularly useful case study because its duration (∼150 yr; Thomas et al., 2007) and forcing are constrained by the proxy record, making an achievable target for climate model simulations (Schmidt and LeGrande, 2005). There are still some uncertainties regarding the hypothesized forcing of the event, including the volume of drainage from proglacial Lake Agassiz-Ojibway (hereafter Lake Agassiz; Barber et al., 1999) into the Hudson Bay (northeastern Canada) and the possibility of multiple meltwater pulses from both the lake and the collapsing Laurentide Ice Sheet (Teller et al., 2002; Gregoire et al., 2012). Model sensitivity to some of these uncertainties has been explored elsewhere (Renssen et al., 2001; Wiersma et al., 2006; LeGrande and Schmidt, 2008; Clarke et al., 2009; Wiersma and Jongma, 2010; Wagner et al., 2013). The target of this intercomparison is to use a median value for the forcing of the 8.2 ka event and compare model sensitivity to North Atlantic surface buoyancy anomalies that have precise dating and a duration short enough to make simulations with state-of-the-art coupled climate models feasible (Schmidt and LeGrande, 2005; Thomas et al., 2007; Kobashi et al., 2007).

2 Models and experiments

We compare 8.2 ka experiments completed with three models: the Community Climate System Model version 3 (CCSM), the Goddard Institute for Space Studies (GISS) ModelE-R and LOVECLIM version 1.2. CCSM and ModelE-R are atmosphere–ocean general circulation models (AOGCMs) coupled without flux adjustments. LOVECLIM is an Earth system model of intermediate complexity with its most significant simplifications applied to the atmosphere component (Table 1). These simplifications include clouds that are prescribed and vertical profiles of temperature and specific humidity that are limited by three atmospheric levels. LOVECLIM also employs a freshwater flux correction between the atmosphere and ocean subcomponents that removes excess precipitation from the Arctic and Atlantic and adds it to the North Pacific (Goosse et al., 2010).

Of relevance to this study, the ocean models of ModelE-R and LOVECLIM are mass-conserving, in which the addition of freshwater causes a rise in the free surface of the ocean and reduces salinity purely through dilution. The ocean model component of CCSM uses the rigid-lid approximation, which does not permit vertical motion at the top of the ocean and parameterizes the addition of freshwater as a salt extraction while keeping the volume of the ocean constant. Yin et al. (2009) discuss the differences between these two approaches and compare results from two versions of the GFDL CM2.1 model using each formulation. For a large freshwater forcing that is similar in magnitude to that used in 8.2 ka experiments, the rigid-lid version exaggerates the forcing and there are significant regional biases in sea surface salinity (SSS). Despite this, the AMOC behaves similarly in the two versions and many fundamental aspects of the two simulations are qualitatively similar.

Boundary conditions specified for the control simulations are listed in Table 2. Early Holocene orbital forcing increased the seasonality of insolation in the Northern Hemisphere and decreased seasonality in the Southern Hemisphere relative to the present (Berger, 1978). Greenhouse gas concentrations for the early Holocene were nearly identical to those for the recent pre-industrial period (Flückiger et al., 2002; Monnin et al., 2004). Two of the control simulations, $CCSM_{all}$ and LOVECLIM, incorporated the surface albedo and elevation effects of the remnant of the Laurentide Ice Sheet that was present near Hudson Bay at 8.5 ka, as reconstructed by Peltier (2004). These same control simulations also included a small (∼0.05 Sv) background flux of Laurentide meltwater (Licciardi et al., 1999). In $CCSM_{all}$, this freshwater flux was added to the modeled St. Lawrence River (Canadian/US Great Lakes Basin) at its outflow, and was spread as a virtual salinity flux along the coast near the river's mouth. In LOVECLIM, the freshwater was added

Table 2. Boundary conditions for control simulations.

Simulation	Orbital parameters	Greenhouse gas concentrations	Ice sheet	Background meltwater flux
$CCSM_{og}$	8.5 ka	$CO_2 = 260$ ppm $CH_4 = 660$ ppb $N_2O = 260$ ppb	none	none
$CCSM_{all}$	8.5 ka	$CO_2 = 260$ ppm $CH_4 = 660$ ppb $N_2O = 260$ ppb	ICE-5G	0.05 Sv added to St. Lawrence River
ModelE-R	1880 AD	$CO_2 = 285$ ppm $CH_4 = 791$ ppb $N_2O = 275$ ppb	none	none
LOVECLIM	8.5 ka	$CO_2 = 260$ ppm $CH_4 = 660$ ppb $N_2O = 260$ ppb	ICE-5G	0.05 Sv added to Hudson Strait

as a volume to the upper layer of the ocean at the Hudson Strait. Since the ocean model in LOVECLIM has a free surface, this effectively means that the surface height was raised. The temperature of the added freshwater in LOVECLIM was assigned the same temperature as the water in the ocean cell to which it was added. Both of these control simulations with background meltwater flux were integrated until reaching a quasi-equilibrium, in which SSS of the North Atlantic had stabilized. Global mean ocean salinity decreases slowly throughout these control simulations due to the background meltwater flux, a trend that parallels observed freshening since the Last Glacial Maximum (Adkins et al., 2002). A second CCSM control simulation ($CCSM_{og;}$ OG = orbital and greenhouse gas only) without a Laurentide Ice Sheet and background meltwater flux is included in this study for a more direct comparison to ModelE-R results.

For the 8.2 ka event experiments, a meltwater pulse (MWP) of 2.5 Sv for 1 yr was added to each of the control simulations to represent the previously-mentioned drainage of Lake Agassiz. This freshwater volume was the best estimate for the drainage event based on flood hydrograph simulations (Clarke et al., 2004). Following the one-year perturbation, the MWP ceased and the climate was allowed to recover. In the models with a free-surface ocean, the MWP was added as a volume to a limited number of grid cells. In ModelE-R, freshwater was added to the approximately 20 grid boxes in the Hudson Bay and was assigned a temperature of 0 °C. In LOVECLIM, freshwater was added to the upper layers of the ocean at the Hudson Strait and was assigned the same temperature as the water in the ocean cell to which it was added. The virtual salinity flux in CCSM required a larger area for the MWP (50–65° N, 35–70° W).

The control simulation for ModelE-R displayed a number of transient, quasi-stable states with either strong or weak AMOC (LeGrande et al., 2006; LeGrande and Schmidt, 2008). For this study, we use an experiment begun from a period of weak AMOC. The weak case was chosen because it exhibited the longest response to the 2.5 Sv × 1 yr forcing, and because it may more closely emulate the early Holocene than periods with strong AMOC since it lacks deep convection in the Labrador Sea between Canada's Labrador coast and Greenland (see LeGrande and Schmidt, 2008 for further detail). Since the weak case exhibits some high amplitude decadal variability, we examined "decadal" results for this model (i.e., the 10-yr mean of the MWP experiment less the 30-yr mean of the closest control years) in order to more clearly show the transient response to the MWP.

We calculated the Student's *t* test for the differences between control and MWP experiments for the two models with annual output (i.e., LOVECLIM and CCSM). Since annual output is no longer available from the ModelE-R experiments and resources do not exist to re-run these simulations, we are unable to make statements about the statistical significance of the model's response to the MWP, about the skill of the model on the annual time-scale and about the relative amplitude of decadal and annual variability. The model simulations in the present study are an "ensemble of opportunity", meaning that most were completed before this intercomparison was planned. One limitation of not coordinating experiments is that perfect comparisons are sometimes impossible to make. However, the main conclusions of this paper would not change were annual data available from all simulations and ensembles of opportunity are important for informing future coordinated intercomparisons.

3 Response to freshwater forcing

3.1 AMOC

AMOC intensity is defined here as the maximum of the Atlantic overturning streamfunction excluding the surface (<500 m) wind-driven overturning circulation. Mean values for the control simulations range from 16 to 20 Sv (Fig. 1), and interannual variability is small in the three simulations

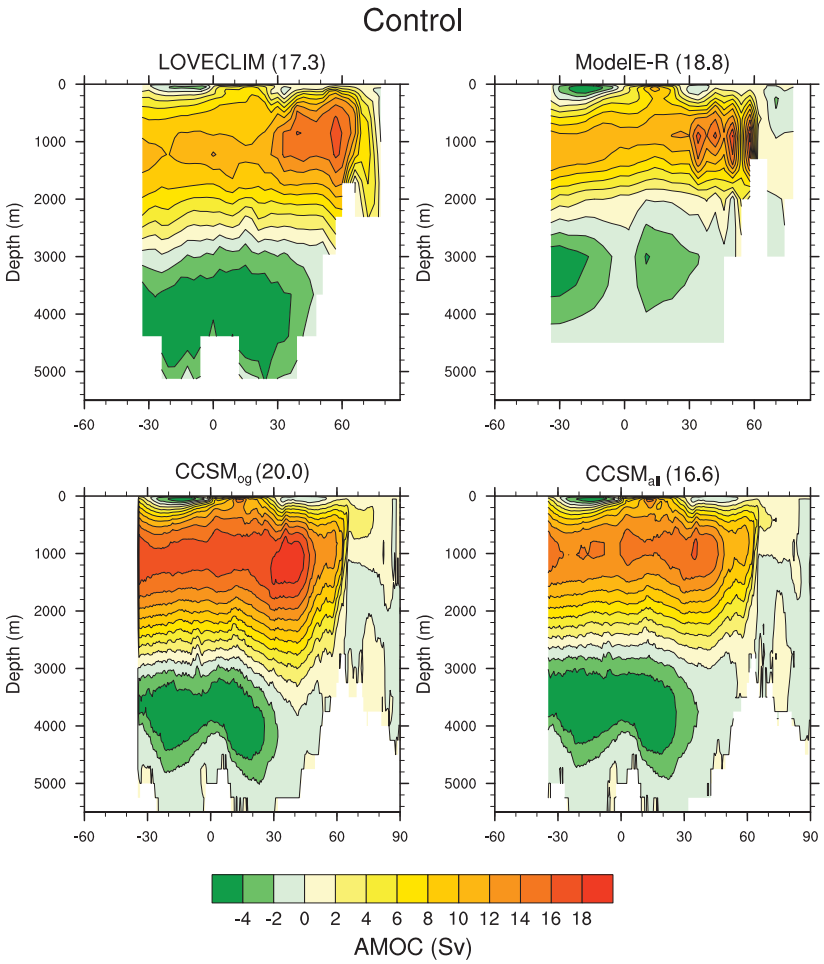

Fig. 1. The Atlantic meridional overturning streamfunctions of the control simulations (see Table 2), in Sv ($1\,\mathrm{Sv} = 10^6\,\mathrm{m}^3\,\mathrm{s}^{-1}$). Plotted values are 200 yr means except for $\mathrm{CCSM_{og}}$, which is a 150 yr mean. Values in parentheses following the model names are long-term means for the maximum of the streamfunction below 500 m water depth.

with available annual output (standard deviations: LOVECLIM = 0.7, $\mathrm{CCSM_{og}} = 1.1$, $\mathrm{CCSM_{all}} = 0.9$ Sv). AMOC intensity is lower by several Sv in the simulations with a background meltwater flux. AMOC has a similar structure in all the control simulations. The northward flow of warm, salty water occurs in the upper 1000 m, while the southward return flow of North Atlantic Deep Water occurs between 1000–3000 m. The anticlockwise cell in the deep ocean, associated with Antarctic Bottom Water formation, has a strength of about 4 Sv in all control simulations.

The values of AMOC intensity in the control simulations are generally similar to the strength of the modern-day AMOC (Meehl et al., 2007). Proxy evidence suggests that the strength of the AMOC during the early Holocene was probably not that different from today (Bianchi and McCave, 1999; Hall et al., 2004; Oppo et al., 2003; McManus et al., 2004; Praetorius et al., 2008). There is some proxy evidence for lack of convection and deep water formation in the Labrador Sea during the early Holocene, however (e.g., Hillaire-Marcel et al., 2001; Solignac et al., 2004; Fagel et al., 2004). To reconcile a vigorous AMOC with lack of Labrador Sea convection, some other convection area, perhaps in the Irminger Basin, might have been stronger in the early Holocene to offset the weaker Labrador Sea convection (Hall et al., 2010).

The location and strength of convection areas in the North Atlantic varies significantly among the control simulations (Fig. 2). Convection occurs primarily in the Nordic Seas in one of the models (LOVECLIM), primarily in the Irminger Sea in another (ModelE-R), and in both the Nordic Seas and just east of the Labrador Sea in the third model (CCSM). Notably, the background meltwater flux of 0.05 Sv does not shut down convection just east of the Labrador Sea in the $\mathrm{CCSM_{all}}$ control simulation (Fig. 2), as that flux is routed to the south of the Labrador Sea by ocean surface currents.

Following the 2.5 Sv MWP for one year, AMOC intensity decreases in all simulations (Fig. 3). The maximum decadal-mean decline in LOVECLIM and CCSM is about 10 %,

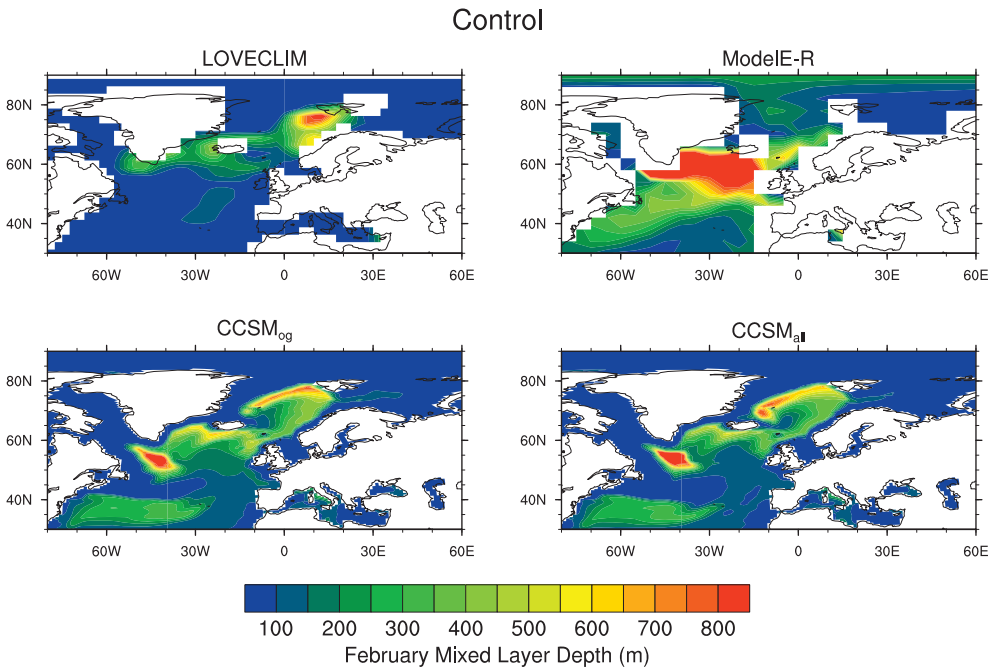

Fig. 2. Control values of February mixed layer depth, in meters. Plotted values are 100 yr means.

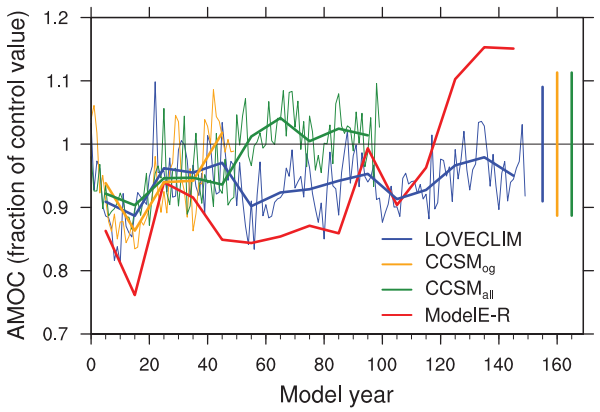

Fig. 3. Time series of AMOC intensity anomalies following the MWP, expressed as a fraction of the long-term control mean. The MWP of 2.5 Sv for one year was added at Model year 1. AMOC intensity is defined as the maximum value of the overturning streamfunction below 500 m water depth (excludes shallow wind-driven overturning). Heavy lines are decadal averages. Vertical lines on the right show the 2-sigma range of interannual variability in the control simulations, and are not shown for ModelE-R since only 30 yr control averages are available.

while for ModelE-R it is about 25 %. The decline in AMOC intensity in LOVECLIM and CCSM is relatively short-lived, on the order of several decades, and generally within the range of natural variability of AMOC in their control simulations. Similarly, mixed-layer depths shoal significantly following the MWP, but this weakening of convection also lasts several decades or less (not shown). The response in ModelE-R is more pronounced and longer-lived, extending on the order of 100–120 yr. Proxy records do not provide a quantitative estimate of AMOC weakening at 8.2 ka, but do suggest a duration of 100–200 yr (Ellison et al., 2006; Kleiven et al., 2008).

3.2 Ocean salinity and temperature

Significant freshening of the North Atlantic occurs following the MWP in all simulations (Fig. 4). The largest anomalies are generally along the coast of Labrador and are up to 1 psu when averaged over the first fifty years following the MWP. Areas of positive SSS anomalies at the mouth of the St. Lawrence River in CCSM$_{all}$ are caused by cessation of the 0.05 Sv background meltwater flux once Lake Agassiz has drained. Globally, negative anomalies greater than 0.2 psu are confined to the North Atlantic and Arctic oceans (not shown).

Patterns of SSS anomalies suggest that freshwater travels eastward from the Labrador Sea into the North Atlantic in all simulations. For most of the simulations, SSS decreases in both the Greenland-Iceland-Norwegian Seas and in the subtropical gyre. This pathway is different from that inferred by Keigwin et al. (2005), who used δ^{18}O of planktic foraminifera to suggest salinity was decreased near Cape Hatteras around 8.2 ka. Also, it has been argued that freshwater released from Hudson Strait would not reach the Nordic Seas, instead being trapped along the North American coast (e.g., Wunsch, 2010) or circulating in the subtropical gyre

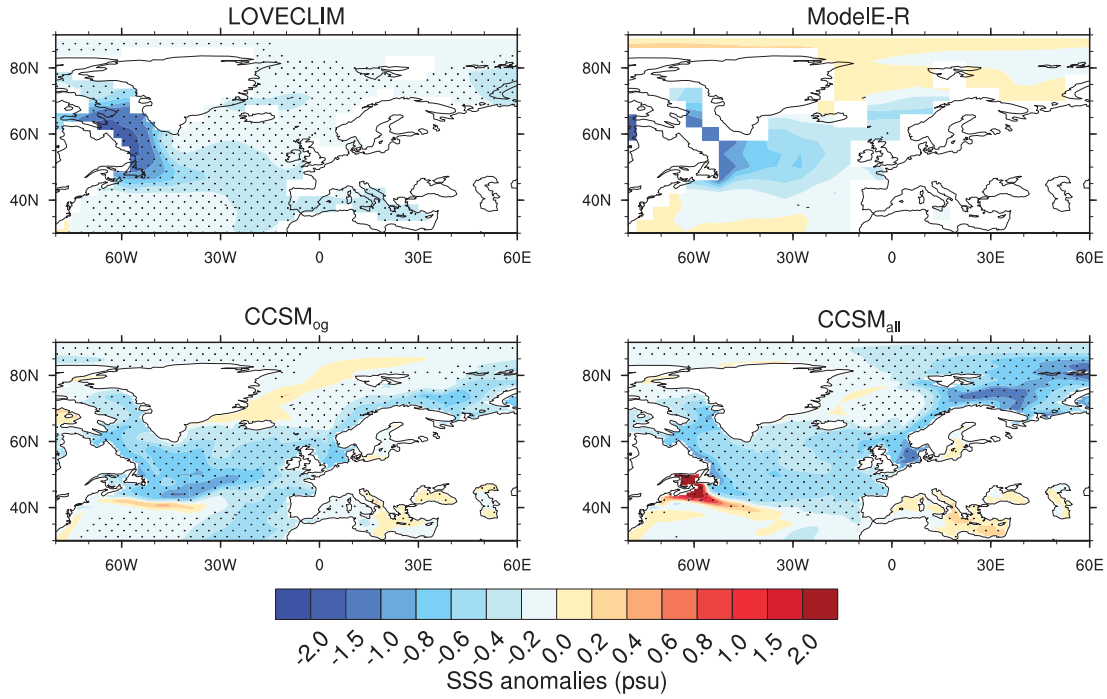

Fig. 4. Anomalies of annual-mean sea surface salinity in the first fifty years following the MWP relative to the control simulation, in practical salinity units. Stippling shows statistical significance at the 95 % level according to a Student's *t* test. Statistical tests were not performed for ModelE-R since only decadal averages were available.

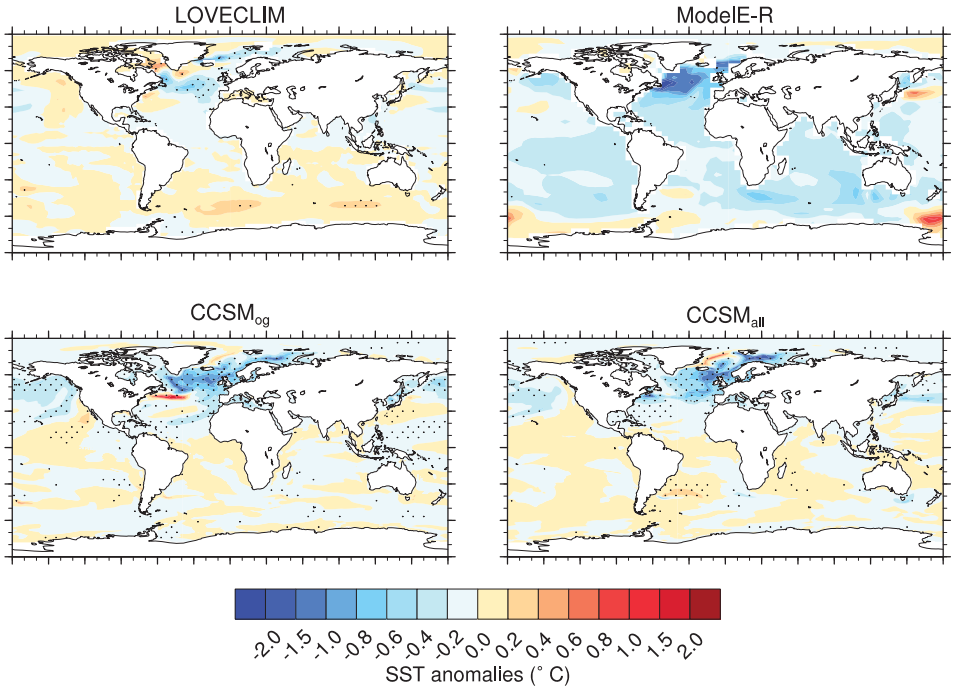

Fig. 5. Anomalies of annual-mean sea surface temperature in the first fifty years following the MWP relative to the control simulation, in degrees Celsius. Stippling shows statistical significance at the 95 % level according to a Student's *t* test. Statistical tests were not performed for ModelE-R since only decadal averages were available.

(Condron and Winsor, 2011). However, several proxy records from the Irminger and Labrador Seas combine δ^{18}O and Mg/Ca of planktic foraminera to infer decreases in δ^{18}O of seawater at 8.2 ka of up to 1 ‰ (Came et al., 2007; Thornalley et al., 2009; Ellison et al., 2006; Winsor et al., 2012; Hoffman et al., 2012), which would be equivalent to a freshening of ∼0.7 psu assuming the Laurentide Ice Sheet meltwater was about −25 ‰ (Hillaire-Marcel et al., 2007). Also, the location of detrital carbonate layers deposited around 8.2 ka indicate greater freshwater transport in the outer branch of the Labrador Current, which typically mixes with the North Atlantic Current and travels to the Nordic Seas (Lewis et al., 2012). The model simulations presented here, as well as others published by Born and Levermann (2010) and Spence et al. (2008), tend to support some amount of freshwater transport into the Nordic Seas.

Likewise, sea surface cooling is concentrated in the North Atlantic in all simulations (Fig. 5). Mean anomalies across the North Atlantic for the first fifty years following the MWP are on the order of 1 °C, though they exceed 2 °C locally in the CCSM and ModelE-R experiments. Maximum anomalies in the LOVECLIM simulation are on the order of ∼0.5 °C and are located in the far North Atlantic. ModelE-R shows cooling on the order of several tenths of a degree Celsius across most of the Southern Hemisphere. The other simulations show little significant change south of 30° N with the exception of $CCSM_{all}$, which has some significant warming in the south Atlantic.

3.3 Barotropic streamfunction

A common model diagnostic for the ocean circulation, including the strengths of the subtropical and subpolar gyres in the North Atlantic, is the vertically-integrated mass transport (barotropic) streamfunction. Values for this quantity are available for three of the simulations (Fig. 6). In these three simulations, transports in both the subtropical gyre and the subpolar gyre weaken for a few decades following freshwater forcing. This result is consistent with the concept that reduction of deep convection in the core of the subpolar gyre, as occurs briefly in these simulations in the Labrador and/or Irminger Seas, weakens this circulation (e.g., Häkkinen and Rhines, 2004). The barotropic streamfunction is not available as standard output for the fourth simulation (LOVECLIM) and is not easily calculated offline. Neither deep convection (Sect. 3.1) nor upper-ocean velocities (top 100 m, not shown) in this model show a large or long-term change forced by the MWP, though, suggesting that the response of the gyres is at least qualitatively similar to the other models.

On the other hand, Born and Levermann (2010) found a prolonged strengthening of the subpolar gyre circulation in a simulation of the 8.2 ka event with the CLIMBER-3α model. In this model, a reduction of deepwater formation in the Nordic Seas intensified the subpolar gyre and triggered internal feedbacks to increase and maintain deep convection in the Labrador Sea. If true, this could explain the onset of deepwater formation in the Labrador Sea around the time of the 8.2 ka event (e.g., Hillaire-Marcel et al., 2001). The different response in CLIMBER-3α might be explained by the fact that the freshwater perturbation had less of a direct impact on the Labrador Sea convection region and instead had greater advection to the Nordic Seas (Born and Levermann, 2010).

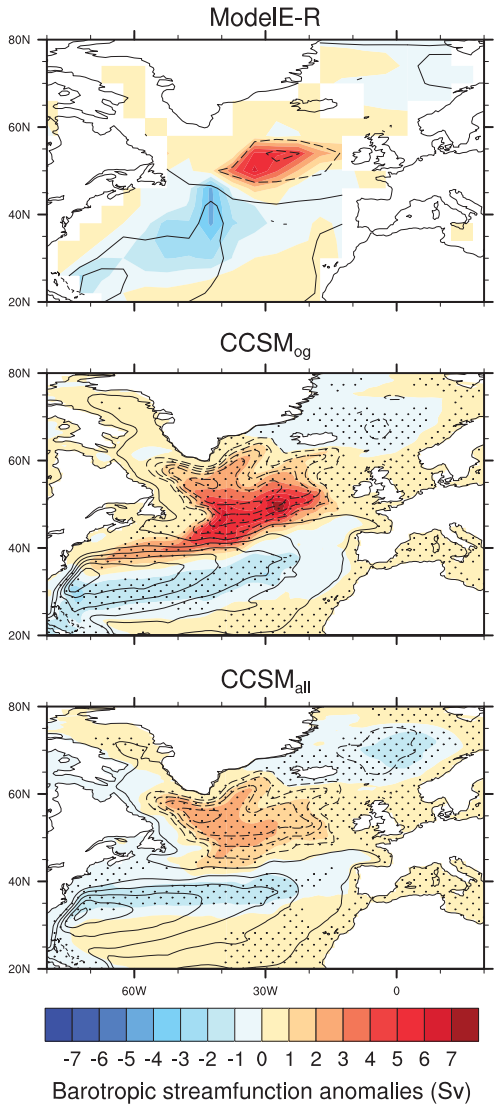

Fig. 6. Control values for barotropic streamfunction (contour lines) and streamfunction anomalies in the first fifty years following the MWP relative to the control simulation, in Sv (colored contours). The contour interval for the control values is 10 Sv. Dashed lines show negative streamfunction values, or a cyclonic circulation. Positive (negative) anomalies for a cyclonic (anticyclonic) circulation indicate weakening of the transport. Stippling shows statistical significance for anomalies at the 95 % level according to a Student's *t* test. Statistical tests were not performed for ModelE-R since only decadal averages were available.

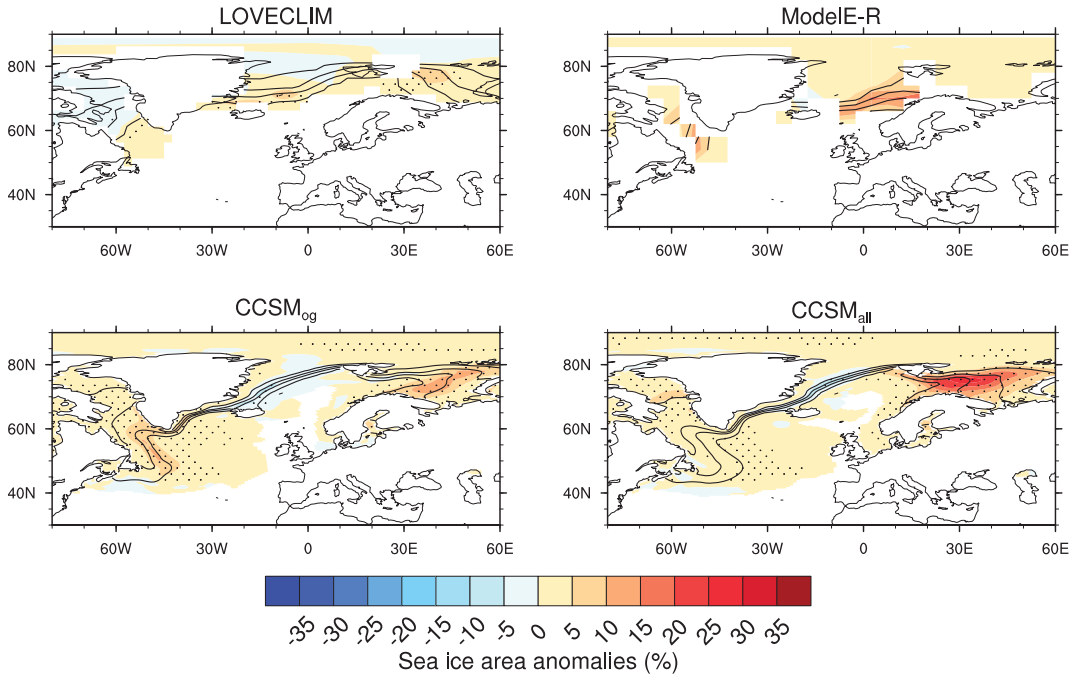

Fig. 7. Control values (contour lines) and anomalies of annual-mean sea ice area in the first fifty years following the MWP relative to the control simulation (colored contours), in percent. The contour lines show values of 5 %, 25 %, 50 % and 75 %. Stippling shows statistical significance at the 95 % level according to a Student's *t* test. Statistical tests were not performed for ModelE-R since only decadal averages were available.

3.4 Sea ice

All of the simulations have areas of significantly expanded sea ice following freshwater forcing, particularly in the Labrador Sea and in the Norwegian and/or Barents Sea (Fig. 7). Generally, these changes for the first fifty years following the MWP are on the order of 5–10 %, although they can be as large as 20–25 % in some areas. Sea ice changes in the Southern Ocean have a heterogeneous spatial pattern and generally are not statistically significant.

3.5 Surface air temperature

The North Atlantic region and the Arctic become significantly colder in most simulations during the first fifty years following the MWP, with mean annual temperatures in the multi-model ensemble decreasing less than ∼0.5 °C over Europe and ∼1.0 °C over Greenland (Fig. 8). These results hold for individual ensemble members, as well, for both Europe (40° N–60° N, 10° W–30° E; anomalies are LOVECLIM = 0.0 °C, CCSM$_{og}$ = −0.3 °C, CCSM$_{all}$ = −0.5 °C, ModelE-R = −0.6 °C) and Greenland (60° N–80° N, 60° W–20° W; anomalies are LOVECLIM = 0.0 °C, CCSM$_{og}$ = −0.6 °C, CCSM$_{all}$ = −0.4 °C, ModelE-R = −0.8 °C). Temperature changes are minimal in the tropics and the Southern Hemisphere. This spatial pattern agrees well with proxy records, which clearly indicate colder conditions across the Northern Hemisphere during the 8.2 ka event but suggest that any Southern Hemisphere temperature changes were likely regional (Fig. 8).

The magnitude of circum-North Atlantic temperature changes inferred from proxies is somewhat larger than those in the models. Temperature reconstructions from pollen and δ^{18}O in Europe consistently show anomalies of about −1.1 to −1.2 °C in mean annual temperature during the 8.2 ka event, although standard errors of these reconstructions are nearly as large as the anomalies themselves (Veski et al., 2004; von Grafenstein et al., 1998; Sarmaja-Korjonen and Seppä, 2007; Feurdean et al., 2008). Nitrogen isotopes from Greenland indicate temperatures decreased about 2.2 °C averaged over the duration of the event, with an even larger decrease of 3.3 °C during the most extreme 60 yr period (Kobashi et al., 2007).

Anomalies over the North Atlantic in the LOVECLIM and CCSM experiments are short-lived; generally, temperature values are outside the range of natural variability (defined as the mean ±2 standard deviations of the control) for less than two decades (Fig. 9). Anomalies are longer-lived in the ModelE-R simulation, lasting on the order of 100 yr. These longer-lived anomalies are a better match to high-resolution proxy records from Europe and Greenland, which consistently show an event duration of 100 to 150 yr (Morrill et al., 2013).

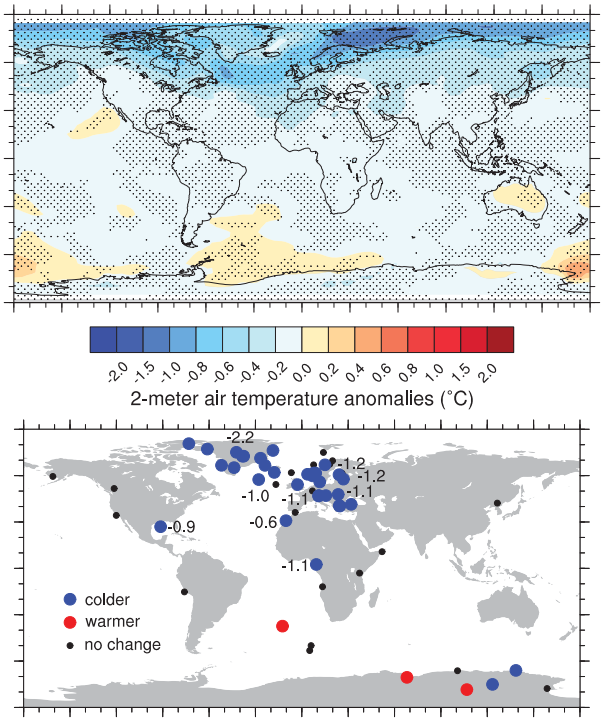

Fig. 8. (Top) Multi-model ensemble mean anomalies of annual-mean 2-meter air temperature in the first fifty years following the MWP relative to the control simulations, in degrees Celsius. Stippling shows grid cells where at least three of the simulations agree on the sign of the temperature anomaly. (Bottom) Qualitative and quantitative mean-annual temperature anomalies relative to the early Holocene background climate, in degrees Celsius, inferred from proxy records for the 8.2 ka event, as summarized by Morrill et al. (2013).

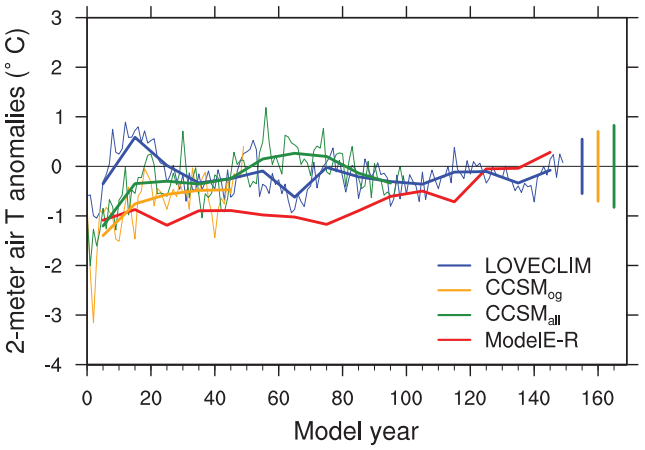

Fig. 9. Time series of annual-mean surface air temperature averaged over the region 50–70° N, 60° W–10° E in the North Atlantic, expressed as anomalies in degrees Celsius from the long-term control average. The MWP of 2.5 Sv for one year was added at Model year 1. Vertical lines on the right show the 2-sigma range of interannual variability in the control simulations, and are not shown for ModelE-R since only 30-yr control averages are available.

3.6 Precipitation

Despite the noise inherent in precipitation, a number of features are common among the model simulations for the fifty years following the MWP. In all cases, the most important changes are a reduction in precipitation over the North Atlantic and Northern Hemisphere tropics, and an increase in precipitation over the Southern Hemisphere tropics (Fig. 10). The tropical pattern, consistent with a southward shift of the mean position of the Intertropical Convergence Zone, is clearest over the Atlantic Ocean (Fig. 11). Tropical proxy records from both speleothem δ^{18}O measurements and indicators of lake water balance support this spatial pattern (Fig. 10).

Several quantitative estimates of drying exist from proxies in high northern latitudes; these include an ∼8 % reduction in accumulation in central Greenland ice cores and an ∼17 % reduction in rainfall inferred from pollen north of the Mediterranean, although again the standard errors of these reconstructions are nearly as large as the anomalies themselves (Feurdean et al., 2008; Pross et al., 2009; Hammer et al., 1997; Rasmussen et al., 2007). The model simulations generally match the magnitude of drying in central Greenland, but typically do not match either the direction or magnitude of change in southeastern Europe. Additionally, evidence for wetter conditions at 8.2 ka from pollen and lake geochemical records in northern Europe is not matched by the freshwater experiments (Fig. 10).

4 Discussion and conclusions

To summarize, the models generally do a good job in reproducing large-scale patterns of temperature and precipitation changes at 8.2 ka inferred from proxy records. These patterns include cooling across most of the Northern Hemisphere and a southward shift of the Intertropical Convergence Zone. The models have less success in matching the magnitude and duration of climate anomalies. Temperature changes in the multi-model ensemble are about half the size of those of quantitative proxy records from Europe and Greenland. For all but one of the simulations, the duration of the 8.2 ka climate anomalies is on the order of several decades rather than the ∼150 yr observed in proxy records. Also, there are discrepancies between model and data for some regional-scale anomaly patterns, including precipitation changes in Europe. These patterns are less well-constrained by proxy evidence, however.

The background climate state of the early Holocene, and the location of convection areas in the North Atlantic more specifically, might explain some of the differences we see between models and proxy data. The ModelE-R simulation has the best match to proxies for event duration, and it has

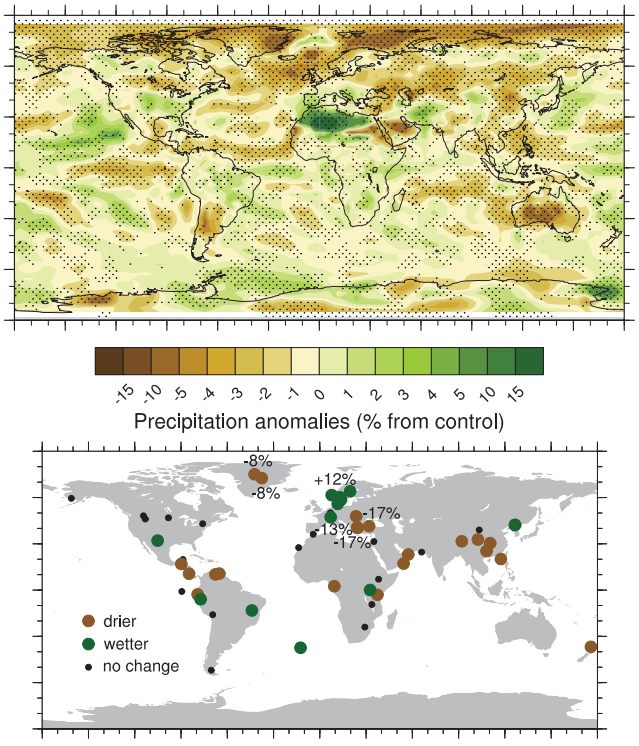

Fig. 10. (Top) Multi-model ensemble mean anomalies of annual-mean precipitation in the first fifty years following the MWP relative to the control simulations, in % change from control. Stippling shows grid cells where at least three of the simulations agree on the sign of the precipitation anomaly. (Bottom) Qualitative and quantitative annual-mean precipitation anomalies, in % change from early Holocene background climate, inferred from proxy records for the 8.2 ka event, as summarized by Morrill et al. (2013).

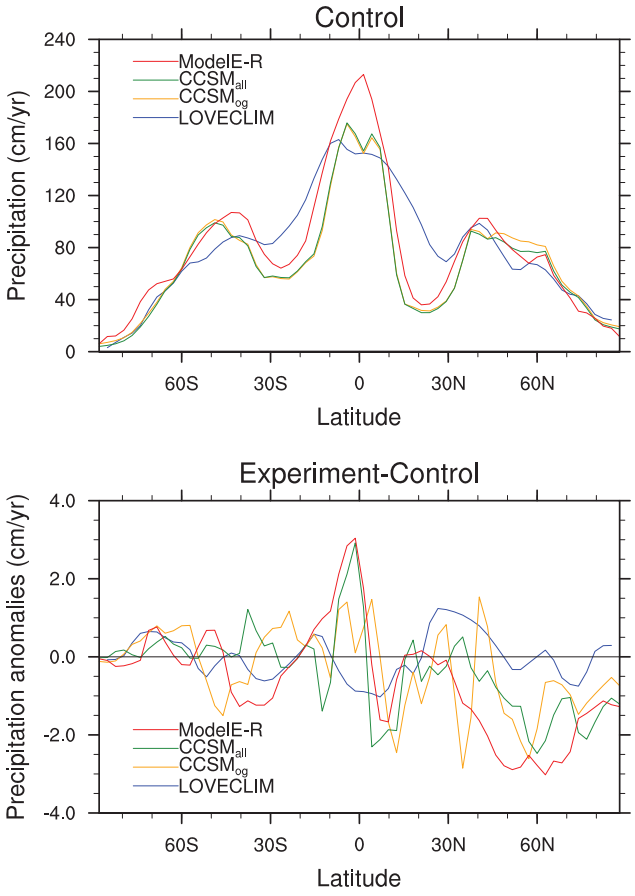

Fig. 11. (Top) Annual-mean precipitation zonally-averaged across the Atlantic (90° W–40° E) in the control simulation, in cm yr^{-1}. (Bottom) Anomalies of Atlantic annual-mean precipitation for the first fifty years following the MWP relative to the control simulation, in cm yr^{-1}.

been previously demonstrated for this model that the lack of Labrador Sea convection is essential for this response (LeGrande and Schmidt, 2008; LeGrande et al., 2006). Previous work with the ECBilt-CLIO model also supports this interpretation; when Labrador Sea convection is weakened by the background meltwater flux, the ocean's ability to transport freshwater anomalies away from the North Atlantic is diminished and the response to freshwater forcing is prolonged (Wiersma et al., 2006). On the other hand, lack of convection in the Labrador Sea does not lead to a long-lived climate response in this model's successor, LOVECLIM. While the exact reasons for this have yet to be determined, the background meltwater flux used in the LOVECLIM experiment is less than that in the ECBilt-CLIO experiments (0.05 vs. 0.17 Sv; Wiersma et al., 2006; Li et al., 2009), and it seems that LOVECLIM is also less sensitive to freshwater perturbations than its predecessor. Also adding uncertainty to the importance of convection strength in the Labrador Sea, proxies indicate that AMOC strength was not too different from today during the early Holocene. In this case, some other convection area, perhaps in the Irminger Basin (between Greenland and Iceland), might have been stronger in the early Holocene to offset the weaker Labrador Sea convection (Hall et al., 2010). If this was true, the strengthened convection areas elsewhere might be able to compensate for decreased freshwater divergence in the Labrador Sea.

Another factor in the model-data mismatch could be the size or the complexity of the MWP. The model simulations were forced with 2.5 Sv for one year, which was the best estimate of the flood hydrograph simulations of Clarke et al. (2004). As these authors point out, though, the total volume of Lake Agassiz could have generated twice this forcing and more complex multipulse patterns are possible (Teller et al., 2002). Their flood model generates a stable drainage channel that prohibits complete drainage, but this result might be unlikely for an outburst flood from Lake Agassiz. In addition, uncertainties in the reconstructed position of the ice-margin on the northern side of Lake Agassiz translate into a range of possible lake volumes spanning 45–200 % of the best estimate (Tornqvist and Hijma, 2012).

Reconstructions of sea level rise at 8.2 ka support the idea of a larger freshwater drainage. Using peat deposits from the Mississippi River delta (US), Li et al. (2012) reconstructed a total eustatic sea level rise of 0.8 to 2.2 m at 8.2 ka. Another reconstruction from the Rhine-Meuse delta (the Netherlands and Belgium) implies a sea level rise of 3.0 ± 1.2 m (Hijma and Cohen, 2010). These are significantly larger than the forcing of 2.5 Sv for one year ($\sim$0.2 m sea level equivalent) or even than the best estimate of the entire volume of Lake Agassiz ($\sim$0.4 m sea level equivalent). Recent model simulations suggest that the collapse of the Laurentide ice-sheet saddle around 8.2 ka provided this larger volume of freshwater (Gregoire et al., 2012), and that this forcing results in a cooling event that matches many proxy records (Wiersma and Jongma, 2010; Wagner et al., 2013).

The difference in boundary conditions between the control simulations does not obviously account for divergent model responses. As shown in the comparison of the two CCSM simulations, $CCSM_{og}$ and $CCSM_{all}$, the addition of a remnant Laurentide Ice Sheet and a background meltwater flux does not alter the model response to freshwater forcing, either in magnitude or duration. It is worth noting, however, that these boundary conditions were important in previous experiments with ECBilt-CLIO for prolonging the AMOC response to Lake Agassiz drainage (Wiersma et al., 2006). Thus, the effects of these boundary conditions might be very model-dependent. Differences between early Holocene and preindustrial orbital forcing and greenhouse gas concentrations are relatively minor, and are not expected to have an important influence. This should be verified, though, with additional model experiments.

Another explanation for the model-data discrepancies is that the models are not sensitive enough to freshwater perturbations. If true, this finding would have important implications for future climate projections, particularly as models suggest that continued melting of the Greenland Ice Sheet at its current rate will have a significant impact on the AMOC (Hu et al., 2009). There are few model intercomparisons to determine whether the sensitivity of these three models to freshwater perturbations is representative of coupled climate models as a whole. For hosing experiments of 0.1 Sv for 100 yr under modern boundary conditions, earlier versions of the CCSM3 (CCSM2) and LOVECLIM (ECBilt-CLIO) have AMOC and surface air temperature responses close to the multi-model ensemble mean (Stouffer et al., 2006). For hosing experiments in a Last Glacial Maximum climate, however, AMOC decreases somewhat less in the CCSM3 and LOVECLIM compared to the multi-model ensemble mean (Kageyama et al., 2012). Improved constraints on the size of freshwater forcing and its location with respect to early Holocene convection areas are necessary to rule out the possibility of inadequate model sensitivity.

Acknowledgements. We thank Lauren Gregoire and an anonymous reviewer for their helpful comments. Funding for the CCSM simulations was provided by grants from the U.S. National Science Foundation, Office of Polar Programs, to CM (ARC-0713951) and BLO-B (ARC-0713971), and supercomputer time was provided by a grant from the National Center for Atmospheric Research (NCAR) Computational Information Systems Laboratory (CISL). CM and BLO-B thank Nan Rosenbloom for running the $CCSM_{all}$ simulations, Ellen Ward for assistance with figures, and Esther Brady and Amy Wagner for helpful discussions. ANL thanks NASA GISS for institutional support. This is Past4Future contribution no. 37. The research leading to these results has received funding from the European Union's Seventh Framework programme (FP7/2007–2013) under grant agreement no 243908, "Past4Future. Climate change – Learning from the past climate."

Edited by: M. Kageyama

References

Adkins, J. F., McIntyre, K., and Schrag, D. P.: The salinity, temperature, and $\delta^{18}O$ of the glacial deep ocean, Science, 298, 1769–1773, 2002.

Barber, D. C., Dyke, A., Hillaire-Marcel, C., Jennings, A. E., Andrews, J. T., Kerwin, M. W., Bilodeau, G., McNeely, R., Southon, J., Morehead, M. D., and Gagnon, J.-M.: Forcing of the cold event of 8,200 years ago by catastrophic drainage of Laurentide lakes, Nature, 400, 344–348, 1999.

Berger, A. L.: Long-term variations of caloric insolation resulting from the Earth's orbital elements, Quaternary Res., 9, 139–167, 1978.

Bianchi, G. G. and McCave, I. N.: Holocene periodicity in North Atlantic climate and deep-ocean flow south of Iceland, Nature, 397, 515–517, 1999.

Born, A. and Levermann, A.: The 8.2 ka event: Abrupt transition of the subpolar gyre toward a modern North Atlantic circulation, Geochem. Geophys. Geosys., 11, Q06011, doi:10.1029/2009GC003024, 2010.

Came, R. E., Oppo, D. W., and McManus, J. F.: Amplitude and timing of temperature and salinity variability in the subpolar North Atlantic over the past 10 k.y., Geology, 35, 315–318, 2007.

Clarke, G. K. C., Leverington, D. W., Teller, J. T., and Dyke, A. S.: Paleohydraulics of the last outburst flood from glacial Lake Agassiz and the 8200 BP cold event, Quaternary Sci. Rev., 23, 389–407, 2004.

Clarke, G. K. C., Bush, A. B. G., and Bush, J. W. M.: Freshwater discharge, sediment transport, and modeled climate impacts of the final drainage of Glacial Lake Agassiz, J. Climate, 22, 2161–2180, 2009.

Collins, W. D., Bitz, C. M., Blackmon, M. L., Bonan, G. B., Bretherton, C. S., Carton, J. A., Chang, P., Doney, S. C., Hack, J. J., Henderson, T. B., Kiehl, J. T., Large, W. G., McKenna, D. S., Santer, B. D., and Smith, R. D.: The Community Climate System Model Version 3 (CCSM3), J. Climate, 19, 2122–2143, 2006.

Condron, A. and Winsor, P.: A subtropical fate awaited freshwater discharged from glacial Lake Agassiz, Geophys. Res. Lett., 38, L03705, doi:10.1029/2010GL046011, 2011.

Ellison, C. R. W., Chapman, M. R., and Hall, I. R.: Surface and deep ocean interactions during the cold climate event 8200 years ago,

Science, 312, 1929–1932, 2006.

Fagel, N., Hillaire-Marcel, C., Humblet, M., Brasseur, R., Weis, D., and Stevenson, R.: Nd and Pb isotope signatures of the clay-size fraction of Labrador Sea sediments during the Holocene: Implications for the inception of the modern deep circulation pattern, Paleoceanography, 19, PA3002, doi:10.1029/2003PA000993, 2004.

Feurdean, A., Klotz, S., Mosbrugger, V., and Wolhfarth, B.: Pollen-based quantitative reconstructions of Holocene climate variability in NW Romania, Palaeogeogr. Palaeoclim., 260, 494–504, 2008.

Flückiger, J., Monnin, E., Stauffer, B., Schwander, J., Stocker, T. F., Chappellaz, J., Raynaud, D., and Barnola, J.-M.: High-resolution Holocene N_2O ice core record and its relationship with CH_4 and CO_2, Global Biogeochem. Cy., 16, 1010, doi:10.29/2001GB001417, 2002.

Goosse, H., Brovkin, V., Fichefet, T., Haarsma, R., Huybrechts, P., Jongma, J., Mouchet, A., Selten, F., Barriat, P.-Y., Campin, J.-M., Deleersnijder, E., Driesschaert, E., Goelzer, H., Janssens, I., Loutre, M.-F., Morales Maqueda, M. A., Opsteegh, T., Mathieu, P.-P., Munhoven, G., Pettersson, E. J., Renssen, H., Roche, D. M., Schaeffer, M., Tartinville, B., Timmermann, A., and Weber, S. L.: Description of the Earth system model of intermediate complexity LOVECLIM version 1.2, Geosci. Model Dev., 3, 603–633, doi:10.5194/gmd-3-603-2010, 2010.

Gregoire, L. J., Payne, A. J., and Valdes, P. J.: Deglacial rapid sea level rises caused by ice-sheet saddle collapses, Nature, 487, 219–223, 2012.

Häkkinen, S. and Rhines, P. B.: Decline of subpolar North Atlantic circulation during the 1990s, Science, 304, 555–559, 2004.

Hall, I. R., Bianchi, G. G., and Evans, J. R.: Centennial to millennial scale Holocene climate-deep water linkage in the North Atlantic, Quaternary Sci. Rev., 23, 1529–1536, 2004.

Hall, I. R., Becker, J., Thornalley, D., and Hemming, S. R.: Holocene variability of North Atlantic deep water: palaeocurrent reconstruction of component water masses close to their source, 10th International Conference on Paleoceanography, La Jolla, CA, 2010.

Hammer, C. U., Andersen, K. K., Clausen, H. B., Dahl-Jensen, D., Hvidberg, C. S., and Iversen, P.: The stratigraphic dating of the GRIP ice core, Special Report of the Geophysical Department, Niels Bohr Institute for Astronomy, Physics and Geophysics, University of Copenhagen, 1997.

Hijma, M. P. and Cohen, K. M.: Timing and magnitude of the sea-level jump preluding the 8200 yr event, Geology, 38, 275–278, 2010.

Hillaire-Marcel, C., de Vernal, A., Bilodeau, G., and Weaver, A. J.: Absence of deep-water formation in the Labrador Sea during the last interglacial period, Nature, 410, 1073–1077, 2001.

Hillaire-Marcel, C., de Vernal, A., and Piper, D. J. W.: Lake Agassiz final drainage event in the northwest North Atlantic, Geophys. Res. Lett., 34, L15601, doi:10.1029/2007GL030396, 2007.

Hoffman, J. S., Carlson, A. E., Winsor, K., Klinkhammer, G. P., LeGrande, A. N., Andrews, J. T., and Strasser, J. C.: Linking the 8.2 ka event and its freshwater forcing in the Labrador Sea, Geophys. Res. Lett., 39, L18703, doi:10.1029/2012GL053047, 2012.

Hu, A., Meehl, G. A., Han, W., and Yin, J.: Transient response of the MOC and climate to potential melting of the Greenland Ice Sheet in the 21st century, Geophys. Res. Lett., 36, L10707, doi:10.1029/2009GL037998, 2009.

Kageyama, M., Merkel, U., Otto-Bliesner, B., Prange, M., Abe-Ouchi, A., Lohmann, G., Roche, D. M., Singarayer, J., Swingedouw, D., and Zhang, X.: Climatic impacts of fresh water hosing under Last Glacial Maximum conditions: a multi-model study, Clim. Past Discuss., 8, 3831–3869, doi:10.5194/cpd-8-3831-2012, 2012.

Keigwin, L. D., Sachs, J. P., Rosenthal, Y., and Boyle, E. A.: The 8200 yr BP event in the slope water system, western subpolar North Atlantic, Paleoceanography, 20, PA2003, doi:10.1029/2004PA001074, 2005.

Kleiven, H. F., Kissel, C., Laj, C., Ninnemann, U. S., Richter, T. O., and Cortijo, E.: Reduced North Atlantic Deep Water coeval with the Glacial lake Agassiz freshwater outburst, Science, 319, 60–64, 2008.

Kobashi, T., Severinghaus, J. P., Brook, E. J., Barnola, J.-M., and Grachev, A. M.: Precise timing and characterization of abrupt climate change 8200 years ago from air trapped in polar ice, Quaternary Sci. Rev., 26, 1212–1222, 2007.

LeGrande, A. N. and Schmidt, G. A.: Ensemble, water isotope-enabled, coupled general circulation modeling insights into the 8.2 ka event, Paleoceanography, 23, PA3207, doi:10.1029/2008PA001610, 2008.

LeGrande, A. N., Schmidt, G. A., Shindell, D. T., Field, C. V., Miller, R. L., Koch, D. M., Faluvegi, G., and Hoffmann, G.: Consistent simulations of multiple proxy responses to an abrupt climate change event, Proc. Natl. Aca. Sci., 103, 837–842, 2006.

Lewis, C. F. M., Miller, A. A. L., Levac, E., Piper, D. J. W., and Sonnichsen, G. V.: Lake Agassiz outburst age and routing by Labrador Current and the 8.2 cal ka cold event, Quaternary Int., 260, 83–97, 2012.

Li, Y.-X., Renssen, H., Wiersma, A. P., and Törnqvist, T. E.: Investigating the impact of Lake Agassiz drainage routes on the 8.2 ka cold event with a climate model, Clim. Past, 5, 471–480, doi:10.5194/cp-5-471-2009, 2009.

Li, Y.-X., Tornqvist, T. E., Nevitt, J. M., and Kohl, B.: Synchronizing a sea-level jump, final Lake Agassiz drainage, and abrupt cooling 8200 years ago, Earth Planet. Sci. Lett., 315–316, 41–50, 2012.

Licciardi, J. M., Teller, J. T., and Clark, P. U.: Freshwater routing by the Laurentide ice sheet during the last deglaciation, in: Mechanisms of Global Climate Change at Millennial Time Scales, edited by: Clark, P. U., Webb, R. S. and Keigwin, L. D., American Geophysical Union, Washington, DC, 177-201, 1999.

McManus, J. F., Francois, R., Gherardi, J.-M., Keigwin, L. D., and Brown-Leger, S.: Collapse and rapid resumption of Atlantic meridional circulation linked to deglacial climate changes, Nature, 428, 834–837, 2004.

Meehl, G., Stocker, T. F., Collins, W. D., Friedlingstein, P., Gaye, A. T., Gregory, J. M., Kitoh, A., Knutti, R., Murphy, J. M., Noda, A., Raper, S. C. B., Watterson, I. G., Weaver, A. J., and Zhao, Z.-C.: Global Climate Projections, in: Climate Change 2007: The Physical Science Basis. Contribution of Working Group I to the Fourth Assessment Report of the Intergovernmental Panel on Climate Change, edited by: Solomon, S., Qin, D., Manning, M., Chen, Z., Marquis, M., Averyt, K. B., Tignor, M., and Miller, H. L., Cambridge University Press, New York, NY, 747–846, 2007.

Monnin, E., Steig, E. J., Siegenthaler, U., Kawamura, K., Schwander, J., Stauffer, B., Stocker, T. F., Morse, D. L., Barnola, J.-M., Bellier, B., Raynaud, D., and Fischer, H.: Evidence for substantial accumulation rate variability in Antarctica during the Holocene, through synchronization of CO_2 in the Taylor Dome, Dome C and DML ice cores, Earth Planet. Sci. Lett., 224, 45–54, 2004.

Morrill, C., Anderson, D. M., Bauer, B. A., Buckner, R., Gille, E. P., Gross, W. S., Hartman, M., and Shah, A.: Proxy benchmarks for intercomparison of 8.2 ka simulations, Clim. Past, 9, 423–432, doi:10.5194/cp-9-423-2013, 2013.

Oppo, D. W., McManus, J. F., and Cullen, J. L.: Deepwater variability in the Holocene epoch, Nature, 422, 277–278, 2003.

Otto-Bliesner, B. L., Brady, E. C., Clauzet, G., Tomas, R., Levis, S., and Kothavala, Z.: Last Glacial Maximum and Holocene climate in CCSM3, J. Climate, 19, 2526–2544, 2006.

Otto-Bliesner, B. L., Hewitt, C. D., Marchitto, T. M., Brady, E., Abe-Ouchi, A., Crucifix, M., Murakami, S., and Weber, S. L.: Last Glacial Maximum ocean thermohaline circulation: PMIP2 model intercomparisons and data constraints, Geophys. Res. Lett., 34, L12706, doi:10.1029/2007GL029475, 2007.

Peltier, W. R.: Global glacial isostasy and the surface of the ice-age Earth: the ICE-5G (VM2) model and GRACE, Ann. Rev. Earth Planet. Sci., 32, 111–149, 2004.

Praetorius, S., McManus, J. F., Oppo, D. W., and Curry, W. B.: Episodic reductions in bottom-water currents since the last ice age, Nat. Geosci., 1, 449–452, 2008.

Pross, J., Kutthoff, U., Muller, U. C., Peyron, O., Dormoy, I., Schmiedl, G., Kalaitzidis, S., and Smith, A. M.: Massive perturbation in terrestrial ecosystems of the Eastern Mediterranean region associated with the 8.2 kyr B.P. climatic event, Geology, 37, 887–890, 2009.

Rasmussen, S. O., Vinther, B. M., Clausen, H. B., and Andersen, K. K.: Early Holocene climate oscillations recorded in three Greenland ice cores, Quaternary Sci. Rev., 26, 1907–1914, 2007.

Renssen, H., Goosse, H., Fichefet, T., and Campin, J.-M.: The 8.2 kyr BP event simulated by a global atmosphere-sea ice-ocean model, Geophys. Res. Lett., 28, 1567–1570, 2001.

Russell, G. L., Miller, J. R., and Rind, D.: A coupled atmosphere-ocean model for transient climate change studies, Atmos.-Ocean, 33, 683–730, 1995.

Russell, G. L., Miller, J. R., Rind, D., Ruedy, R. A., Schmidt, G. A., and Sheth, S.: Comparison of model and observed regional temperature changes during the past 40 years, J. Geophys. Res., 105, 14891–14898, doi:10.1029/2000JD900156, 2000.

Sarmaja-Korjonen, K. and Seppä, H.: Abrupt and consistent responses of aquatic and terrestrial ecosystems to the 8200 cal. yr cold event: a lacustrine record from Lake Arapisto, Finland, Holocene, 17, 457–467, 2007.

Schmidt, G. A. and LeGrande, A. N.: The Goldilocks abrupt climate change event, Quaternary Sci. Rev., 24, 1109–1110, 2005.

Schmidt, G. A., Ruedy, R., Hansen, J. E., Aleinov, I., Bell, N., Bauer, M., Bauer, S., Cairns, B., Canuto, V., Cheng, Y., Del Genio, A., Faluvegi, G., Friend, A. D., Hall, T. M., Hu, Y., Kelley, M., Kiang, N. Y., Koch, D., Lacis, A. A., Lerner, J., Lo, K. K., Miller, R. L., Nazarenko, L., Oinas, V., Perlwitz, J. P., Perlwitz, J., Rind, D., Romanou, A., Russell, G. L., Sato, M., Shindell, D. T., Stone, P. H., Sun, S., Tausnev, N., Thresher, D., and Yao, M.-S.: Present day atmospheric simulations using GISS ModelE: Comparison to in-situ, satellite and reanalysis data, J. Climate, 19, 153–192, doi:10.1175/JCLI3612.1, 2006.

Schmittner, A.: Decline of the marine ecosystem caused by a reduction in the Atlantic overturning circulation, Nature, 434, 628–633, 2005.

Schmittner, A., Latif, M., and Schneider, B.: Model projections of the North Atlantic thermohaline circulation for the 21st century assessed by observations, Geophys. Res. Lett., 32, L23710, doi:10.1029/2005GL024368, 2005.

Solignac, S., deVernal, A., and Hillaire-Marcel, C.: Holocene sea-surface conditions in the North Atlantic – contrasted trends and regimes in the western and eastern sectors (Labrador Sea vs. Iceland Basin), Quaternary Sci. Rev., 23, 319–334, 2004.

Spence, J. P., Eby, M., and Weaver, A. J.: The sensitivity of the Atlantic meridional overturning circulation to freshwater forcing at eddy permitting resolutions, J. Climate, 21, 2697–2710, 2008.

Stouffer, R. J., Yin, J., Gregory, J. M., Dixon, K. W., Spelman, M. J., Hurlin, W., Weaver, A. J., Eby, M., Flato, G. M., Hasumi, H., Hu, A., Jungclaus, J. H., Kamenkovich, I. V., Levermann, A., Montoya, M., Murakami, S., Nawrath, S., Oka, A., Peltier, W. R., Robitaille, D. Y., Sokolov, A., Vettoretti, G., and Weber, S. L.: Investigating the causes of the response of the thermohaline circulation to past and future climate changes, J. Climate, 19, 1365–1387, 2006.

Teller, J. T., Leverington, D. W., and Mann, J. D.: Freshwater outbursts to the oceans from glacial Lake Agassiz and their role in climate change during the last deglaciation, Quaternary Sci. Rev., 21, 879–887, 2002.

Thomas, E. R., Wolff, E. W., Mulvaney, R., Steffensen, J. P., Johnsen, S. J., Arrowsmith, C., White, J. W. C., Vaughn, B., and Popp, T.: The 8.2 ka event from Greenland ice cores, Quaternary Sci. Rev., 26, 70–81, 2007.

Thornalley, D. J. R., Elderfield, H., and McCave, I. N.: Holocene oscillations in temperature and salinity of the surface subpolar North Atlantic, Nature, 457, 711–714, 2009.

Timmermann, A., An, S.-I., Krebs, U., and Goosse, H.: ENSO suppression due to weakening of the North Atlantic thermohaline circulation, J. Climate, 18, 3122–3139, 2005.

Tornqvist, T. E. and Hijma, M. P.: Links between early Holocene ice-sheet decay, sea-level rise and abrupt climate change, Nat. Geosci., 5, 601–606, 2012.

Vellinga, M. and Wood, R. A.: Global climatic impacts of a collapse of the Atlantic thermohaline circulation, Climatic Change, 54, 251–267, 2002.

Veski, S., Seppä, H., and Ojala, A. E. K.: Cold event at 8200 yr BP recorded in annually laminated lake sediments in eastern Europe, Geology, 32, 681–684, 2004.

von Grafenstein, U., Erlenkeuser, H., Muller, J., Jouzel, J., and Johnsen, S.: The cold event 8200 years ago documented in oxygen isotope records of precipitation in Europe and Greenland, Clim. Dynam., 14, 73–81, 1998.

Wagner, A. J., Morrill, C., Otto-Bliesner, B. L., Rosenbloom, N., and Watkins, K. R.: Model support for forcing of the 8.2 ka event by meltwater from the Hudson Bay ice dome, Clim. Dynam., doi:10.1007/s00382-013-1706-z, online first, 2013.

Wiersma, A. P. and Jongma, J. I.: A role for icebergs in the 8.2 ka climate event, Clim. Dynam., 35, 535–549, 2010.

Wiersma, A. P., Renssen, H., Goosse, H., and Fichefet, T.: Evaluation of different freshwater forcing scenarios for the 8.2 ka BP

event in a coupled climate model, Clim. Dynam., 27, 831–849, 2006.

Winsor, K., Carlson, A. E., Klinkhammer, G. P., Stoner, J. S., and Hatfield, R. G.: Evolution of the northeast Labrador Sea during the last interglaciation, Geochem. Geophys. Geosys., 13, Q11006, doi:10.1029/2012GC004263, 2012.

Wunsch, C.: Towards understanding the Paleocean, Quaternary Sci. Rev., 29, 1960–1967, 2010.

Yin, J., Stouffer, R. J., Spelman, M. J., and Griffies, S. M.: Evaluating the uncertainty induced by the virtual salt flux assumption in climate simulations and future projections, J. Climate, 23, 80–96, 2009.

Zhang, R. and Delworth, T. L.: Impact of Atlantic multidecadal oscillations on India/Sahel rainfall and Atlantic hurricanes, Geophys. Res. Lett., 33, L17712, doi:10.1029/2006GL026267, 2006.